Prediction of the Strain hardening exponent of HP40-Nb alloy

Milica Timotijević[1*], Mišo Bjelić[1], Dragan Rajnović[2], Olivera Erić Cekić[1]

[1]Faculty of Mechanical and Civil Engineering, University of Kragujevac, Kraljevo (Serbia)
[2]Department of Production Engineering, Faculty of Technical Science, University of Novi Sad, Novi Sad (Serbia)

This paper investigate the reliability of the strain hardening exponent calculation methods in the case of HP40-Nb class material. The approach was to analyse which one of the mathematical models (Hollomon, Swift, and Ludwik) could be applied and which provides the most accurate results to obtain the strain hardening exponent of centrifugally cast steel alloy HP40-Nb. The modelling was performed using the values of stress and strain obtained in the experiment by uniaxial tension. It was found that using the Hollomon and Swift methods the best approximation of the strain hardening exponent with theoretical values could be obtained.

Keywords: Mathematical Models, Strain hardening exponent, alloy HP40-Nb

1. INTRODUCTION

The strain-hardening exponent (*n*) and the strength coefficient are basic mechanical behaviour performance parameters of metallic materials. The exponent *n* can be determined from a tension test through appropriate transformations of stress-strain data and least-squares fitting of a straight line. Procedures for the computation of exponent *n* have been standardized by ASTM International and ISO. There are various mathematical models that were developed to represent the stress- strain behaviour of the materials [1].

Many researchers have carried out studies on the modelling of flow curves of materials. Sener et al. [2] have compared different constitutive equations for austenitic stainless 304 and ferritic 430 stainless steel sheets and have recommended the most suitable model for these materials. The models applicable are the Hollomon, Ludwik, Swift and El-Magd, model. Uniaxial tensile tests were carried out to obtain the material constants (strength coefficient and strain hardening coefficient) of the models. Afterwards, the applicability of these models was evaluated by comparing nonlinear regression parameter R^2 and the most suitable model was determined for the tested materials. It was concluded that the maximum plastic strain value of the austenite 304 stainless steel sheet (0.35) is higher than that of the 430 ferritic stainless steel sheet (0.11) in the uniform plastic deformation region. This is expected due to the higher value of the strain hardening coefficient *n* in austenite stainless steel. From the value of statistical parameters R^2, it was concluded that the El-Magd model is highly effective for predicting the stress-strain curve, compared to the other three models. Ludwig model showed the worst performance for both materials.

Samuel et al. [3] have investigated suitability of the different constitutive equations for 316 stainless sheet steels which were prior deformed to 7.5%, 16.2% and 24.7% true plastic strain in uniaxial tension at room temperature. They found that behaviour could be adequately described by Ludwigson type and Swift equation. Further, they concluded that the strain hardening parameters at a given strain rate and temperature show that the strain hardening coefficient is weakly dependent on yield strength while the strain hardening index shows a strong dependence on yield strength.

The results of tensile tests on AISI 1004 steel, AISI 1020 steel, and copper were used for a computer simulation by applying the finite element analysis (FEA) in work of Samuel and Rodriguez [4]. The values of the strength coefficient and the strain hardening exponent were obtained by linear regression using a power function. The results were very similar to those determined in accordance with the ASTM E646-07 standard. Finally, the good correlation between the simulations and the physical tests in the plastic region suggests that the simulation method adopted in this work has significant potential for quick and precise application to the drawing process.

D.F Pinto et al. [5] carried out the transformation of nominal voltage deformation curve into true voltage deformation dependency curve by math method. For the calculation, diagrams of dependency of eight different materials were used: nickel alloy 75, 12% Mn steel, steel S355, stainless steel 316L, alumnium tin alloy AA 1050, aluminum alloy sheet AA 5182, steel sheet dx56, and steel sheet of ZStE. The values for strain hardening coefficient were calculated based on three definitions of strains: true strain, conventional definition of true plastic strain, and true plastic strain according to ISO formula. After that, the values for the strain hardening coefficient were compared and it proposed an alternative formulation in which the strength coefficient and the strain-hardening exponent are functions of true-plastic deformation.

In this paper, a comparative study was carried out on Hollomon, Ludwik and Swift models to describe the flow behaviour of HP40-Nb alloy and validate it through ASTM E 646-16 [6] with the experimental data from the literature.

2. EXPERIMENTAL DETAILS

The materials in this study were machined out of one tube, made of the centrifugally cast alloy HP-40 alloy containing 1.5 wt.% Nb. Chemical composition of the tube samples supplied for investigation was analysed through standard analytical method of optical emission spectrophotometry atI Spark 8860.

*Corresponding author: Milica Timotijević, timotijevic.milica93@gmail.com

The catalytic tubes coming from the hydrogen plant are conventionally labelled as F-1A in this paper. The tube segments with 350 mm in length, were cut from the furnace regions which has been in exploitation for 20 years. Operating condition of the tubes was 870 °C under the maximum internal pressure of 2.5 bars (250 kPa). The exact locations where the sections were cut on the reformer columns in the respective plants were unreported and remain unknown. The tensile test of standard specimens (ISO 6892-1:2009) with a gauge length of 50 mm were carried out at room temperature using universal testing machine Schenck Trebel (1000 kN) under the constant crosshead speed mode wih a nominal strain rate of 2 mm/min.

The specimens for microstructural investigation were polished following standard metallographic procedure and etched using a solution of 15 ml HCl, 10 ml Glycerol, and 5 ml HNO_3. The microstructure was examined using scanning electron microscope JOEL JSM 6460 LV. The phases observed were analysed using an energy dispersive x-ray analyser system (EDS) INCA Oxford Instruments in conjunction with a SEM.

3. RESULTS

The chemical composition of the tube samples is presented in Table 1.

Table 1: Chemical composition (mass. %) of the tube samples

	C	Mn	Si	P	Ni	Cr	Mo	Nb
HP 40	0.45	0.984	1.45	0.04	33.47	25.04	0.03	1.50

The mechanical properties of the experimental samples are shown in Table 2.

The service tube tensile tests demonstrate that the tensile strength decreased from 450 MPa to 358 MPa, the yield strength increased from 240 MPa to 308 MPa, and the elongation decreased from 10% to 4.5%, respectively.

Table 2: The mechanical properties of samples measured by the tensile tests

Material	Ultimate tensile strength [MPa]	0.2%Proof stress [MPa]	Elonga-tion [%]	Hardness HB
As-cast	450	240	10	215
Service tube	358	308	4.5	185

Results of microstructural analysis are given in Figure 1. The microstructure consists of an austenitic matrix and a continuous network of primary eutectic carbides of two types: one rich in Nb (bright particles in Fig.1b) and one rich in Cr (dark particles in Fig.1b). These carbides are NbC and M7C3 (M= Cr, Ni, Fe) type.

The schematic illustration of tensile testing specimen is shown in Figure 2. The uniaxial tensile test is performed on a universal testing machine (Schenck Trebel), in displacement control mode, Figure 3.

The illustration of a True- Stress versus True-Strain curve for the material analysed is shown on Figure 4.

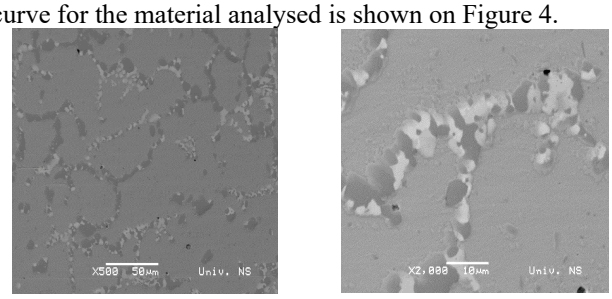

a) *b)*

Figure 1: Microstructure of the HP heat resistant alloy SEM BSE images illustrating cross sections of samples from tube HP at different magnifications

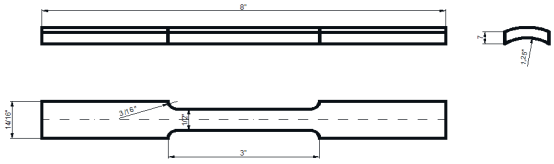

Figure 2: Schematic illustration of a tensile specimen

Figure 3: Photograph of the universal testing machine Schenck Trebel 1000 kN

The illustration of a True- Stress versus True-Strain curve for the material analysed is shown on Figure 4.

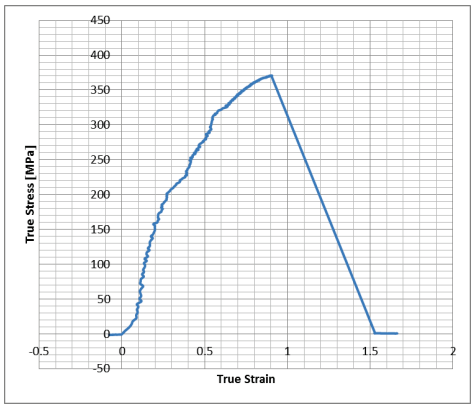

Figure 4: True Stress vs. True Strain Curve of the material analysed

The strain-hardening exponent n was calculated using the standard test method for tensile strain-hardening

exponents of metallic sheet materials (ASTM standard E646-16 [6]).

The equation for calculating n from a linear regression using five points taken in geometrical progression between true strain values of ε = 0.010 and 0.032 is as follows:

$$n = \frac{5\sum_{i=1}^{5}(\log\varepsilon_i \log\sigma_i) - (\sum_{i=1}^{5}\log\varepsilon_i \sum_{i=1}^{5}\log\sigma_i)}{5\sum_{i=1}^{5}(\log\varepsilon_i)^2 - (\sum_{i=1}^{5}\log\varepsilon_i)^2} \quad (2)$$

where σ_i is the true stress and ε_i is the true strain.

The equation for calculating the logarithm of the strength coefficient, K, is as follows:

$$\log K = \frac{\sum_{i=1}^{N}(\log\sigma_i) - n\sum_{i=1}^{N}\log\varepsilon_i}{N} \quad (3)$$

The calculation of the standard deviation of the strain-hardening exponent, SD_n, is based upon the variance of the slope of the regression line.

$$SD_n = \left[\frac{N\sum_{i=1}^{N}(\log\sigma_i - \log K - n\log\varepsilon_i)^2}{(N-2)\left(N\sum_{i=1}^{N}(\log\varepsilon_i)^2 - \left(\sum_{i=1}^{N}\log\varepsilon_i\right)^2\right)}\right]^{1/2} \quad (4)$$

An example of a worksheet for manually calculating these values is found in Appendix 1.

The logarithmized yield stress curve for test tubes is provided in Figure 5.

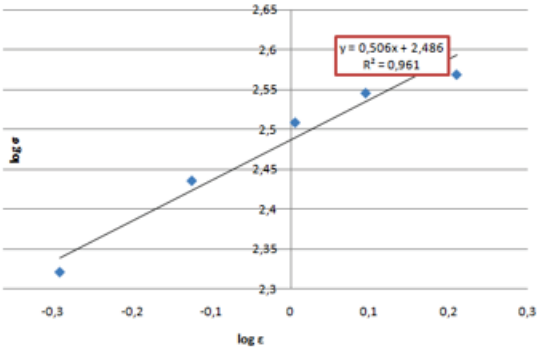

Figure 5: Log σ versus log ε for n and k calculation

The trend line in Figure 5 is linear, i.e., of the type y=ax + *b*, where the coefficient (slope of the line) *a* and the intercept *b* represent the hardening exponent *n* and the strength coefficient *Kσ*, respectively.

The theoretical value for the strain hardening coefficient for the material is n = 0.45-0.55 [10.].

In the logarithmic curve of experimental values (log σ-log ε) the value of the strain hardening coefficient is obtained: *n* = 0,48 for the material analysed.

Based on the presented, it can be concluded that the obtained values of the strain hardening coefficient with the experiment are within the boundaries of theoretical values.

Mathematical modelling on the experimental values of yield stress for the analysed material (numeric and logarithmic) are provided in Table 3.

Table 3: Experimental values of yield stress for the investigated material

point	σ [MPa]	ε [%]
1	209.10	0.5105
2	272.50	0.7501
3	322.63	1.0137
4	351.43	1.2452
5	370.77	1.6228

Mathematical modelling of yield stress (σ-ε) was performed using three equations of considered quai-static models:

- Hollomon equation $\sigma(\varepsilon) = K\varepsilon^n$ [7] (5)

- Ludwik equation $\sigma(\varepsilon) = \sigma_y + K\varepsilon_p^n$ [8] (6)

- Swift equation $\sigma(\varepsilon) = K(\varepsilon_0 + \varepsilon_p)^n$ [9] (7)

Here σ is true stress,σ_y is the yield stress, ε is true plastic strain, K is the strength coefficient, ε_p plastic strain, ε_0 is initial strain, *n* is the strain hardening exponent.

Five different yield stress values σ were used to model yield stress curve σ-ε, as recommended in ASTM E646-16

In the MATLAB program, a simulation of yield stress curve was performed using the specified models (empirical equations).

Three different constitutive models (Hollomon, Ludwick and Swift) are evaluated in this paper. The parameters for such models are identified from experimentally determined flow curves of material by curve fitting techniques.

Comparisons of predicted flow curves by different models with experimental data for the material analysis are shown in Figure 6-8.

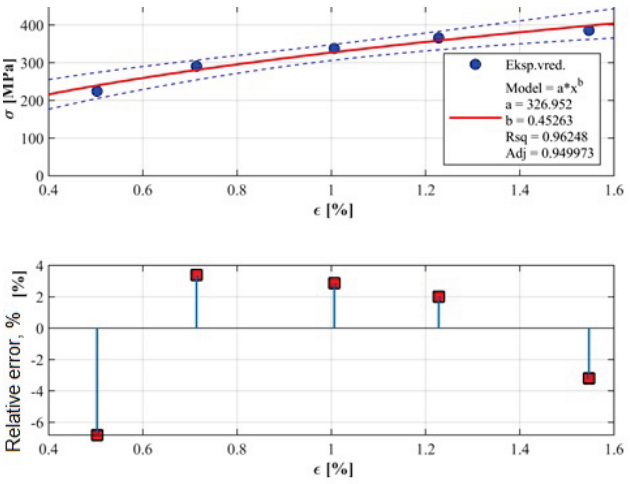

Figure 6: Comparison between the experimentally measured and calculated K and n(a and b in legend) values obtained by Hollomon method

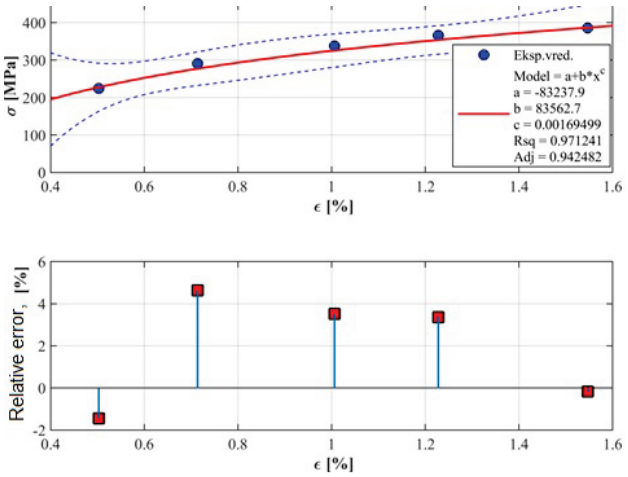

Figure 7: Comparison between the experimentally measured and calculated a (K) and b (n) values obtained by Ludwik method

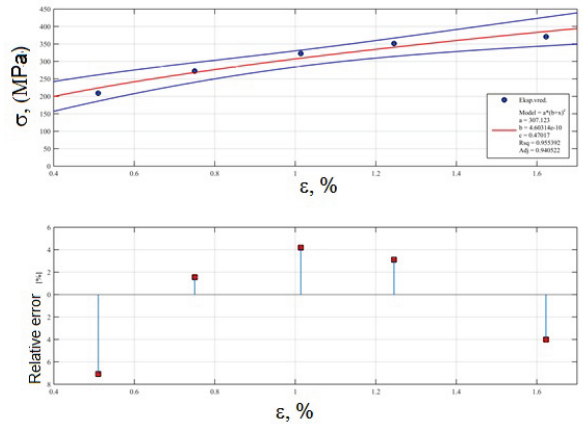

Figure 8: Comparison between the experimentally measured and calculated a (K) and b (n) values obtained by Swift method

Comparing the values of Adj from the legend in Figures 6-8 for the Hollomon, Ludwik and Swift models for the investigated material, we notice that the accuracy of the obtained values for all three models is ≈94%.

The R^2 values of the models for HP40+Nb alloy are shown in Figure 6-8. It can be seen that Swift model is the best model for the prediction of flow curve in the uniform plastic deformation region for the material analysed. In another hand, the Ludwik model although had the highest R^2 values among gives unrealistic values K and n (Table 4) compared to the other models (Hollomon and Swift). This parameter (R^2) is the square of the correlation between the response values and the predicted response values [10].

Total review of theoretical values, experimental values, and strain hardening coefficient values obtained by the simulation in MATILAB, are given in Table 4.

The lowest n values were obtained for the HP40+Nb alloy using Ludwik model.

Table 4: Parameters obtained for the constitutive equations and methodology with ASTM E-646[6], during the characterization of the HP40+Nb alloy

Model	K [MPa]	n	σ_y	ε_0
Hollomon [7]	326.96	0.47		
Ludwik [8]	83562.70	0.002	-83237.9	
Swift [9]	307.12	0.46		4.60314E-10
ASTM E 646[6]	2503.78	0.530		

It can be seen from Table 4, that applying Hollomon and Swift models, the most approximate value to the theoretical value of strain hardening coefficient could be obtained.

4. CONCLUSION

Based on the analysis done and the experimental results, the following conclusions can be made:

- The values of strain hardening coefficient for tested samples obtained using the Hollomon model and Swift model are in c with theoretical values of strain hardening. These two methods proved to be satisfactory for mathematical modelling of the material tested.
- The Ludwik method has shown the worst performance for the material analysed.
- For the material tested it can be concluded that yield stress curve is best described by Hollomon and Swift mathematical models.

ACKNOWLEDGEMENTS

This work is co-financed by the Ministry of Education, Science and Technological Development of the Republic of Serbia on the base of the contract whose record number is 451-03-9/2021-14/200108. The authors thank the Ministry of Education, Science and Technological Development of the Republic of Serbia for supporting this research.

For the continuous support in our experimental work at Military Technical Institute in Belgrade in the Laboratory for Construction and Technical Materials, my thanks go to dr Z. Burzic and dr S. Perkovic.

REFERENCES

[1] A.E. Matusevich, R.Mancini, J. Massa: "Computation of Tensile Strain-Hardening Exponents through the Power-Law Relationship", Journal of Testing and Evaluation, pp. 1-29, (2012)

[2] B, Sener, M.E.Yurci: "Comparison of Quasi-Static Constitutive Equations and Modeling of Flow Curves for Austenitic 304 and Ferritic 430 Stainless Steels"', Special Issue of the 6th International Congress & Exhibition

(APMAS2016),, Istanbul, Turkey, Vol. 131, pp. 605-607 (2017)

[3] K. G. Samuel: “Limitations of Hollomon and Ludwigson stress-strain relations in assessing the strain hardening parameters”, Journal of Physics S: Applied Physics, Vol. 39, pp. 203-212 (2016)

[4] K.G.Samuel, P. Rodriguez: “On power-law type relationships and the Ludwigson explanation for the stress-strain behaviour of AISI 316 stainless steel”,Journal od materials science,Vvol. 40, pp. 5727-5731 (2005)

[5] D.F. Pinto, M.A. Pinto, P.R. Pinto, A. Rodrigues da Costa: “Validation of a simplified computer simulation method for plastic forming of metals by conventional tensile tests”, REM International Engineering Journal, Vol. 70, no 4, pp. 437-443 (2017)

[6] ASTM Standard E 646-16: Standard Test Method for Tensile Strain-Hardening Exponents (n -Values) of Metallic Sheet Materials, ASTM International, West Conshohocken, PA, (2016).

[7] J. Hollomon, Tensile Deformation, Trans AIME, Vol. 32, pp. 268–290 (1945).

[8] . P. Ludwik, Elemente der Technologischen Mechanik, (Verlag Von Julius Springer, Leipzig), p. 32 (1909).

[9] H. J. SWIFT, J. Mech. Phys. Solids **1** p.1 (1952).

[10] D.G. Kleinbaum, L.L. Kupper, Applied Regression Analysis and Other Multivariable Methods, Cengage Learning, Belmont (2007).

APPENDIX

Table X1.1

			B = A x (1+D)	**C= log B**	
		A	B	C	
	Load F	Engineering Stress	True Stress	$Y=\log_{10}$	Y^2
	kN	MPa	MPa		
1	18.150	209.10	211.23	2.324759	5.404504
2	23.653	272.50	276.59	2.441835	5.962559
3	28.004	322.63	329.17	2.517417	6.337389
4	30.504	351.43	360.18	2.556522	6.535803
5	32.183	370.77	382.80	2.582974	6.671756

	D=G/50	**E = ln (1+D)**			
G	D	E	**X=logE**		
Extension	Engineering Strain ε	True Strain ε	$X=\log_{10}\varepsilon$	X^2	X*Y
mm					
0.511	0.010	0.010158	-1.993182	3.972774	-4.633668
0.750	0.015	0.014891	-1.827088	3.338252	-4.461449
1.014	0.020	0.020071	-1.697426	2.881256	-4.273130
1.245	0.025	0.024599	-1.609083	2.589150	-4.113657
1.623	0.032	0.031940	-1.495659	2.236997	-3.863249

N=	**5**	**ΣY=12.423507**	**12.423507**

ΣX= - 8.622439; ΣY²= 30.912012;

ΣX²= 15.018428

ΣXY= -21.345152

A- Values are obtained from Fig.2

B- Area=0.504 x 0.1045=0.052668 in².

C= log B

C-True stress = (engineering stres) x (1+engineering strain) B = A x (1+D)

D- Engineering strain = (extension) / gage length

E- True strain = l n (1 + engineering strain)

E = ln (1+D)

Where: X denotes ε; Y denotes σ, n denotes strain hardening exponent, and b denotes log K

Date operated upon this example are taken from Fig. 2 and evaluated in Table X1.1

The number of data-pairs N is 5

All logarithms used in the example area base 10

From Table X1.1. :

ΣX= Σ(loge)= -8.622439

ΣY= Σ(logσ)=12.423507

ΣX² = 15.018428

$\bar{X} = \frac{\sum X}{N} = -1.724488$

$\sum Y = \sum(log\sigma) = 12.4223507$

$\sum Y^2$= 30.912012

$\bar{Y} = \frac{\sum Y}{N} = 2.484701$

$\sum XY = -21.345152$

The calculations for n and b

$\frac{\sum X * \sum Y}{N}$ = -21.424187

Step 1

$S_{XY} = \sum XY - \frac{\sum X * \sum Y}{N} = \sum XY - \text{Step 1} = 0.079035$

Step2

$\frac{(\sum X)^2}{N} = 14.869292$

Step 3

$S_{XX} = \sum X^2 - \frac{(\sum X)^2}{N} = \sum X^2 - Step\ 3$ =0.149136

Step 4

$n = \frac{S_{xy}}{S_{xx}} = \frac{Step\ 2}{Step\ 4}$ =0.529951

n= 0,530

Step 5

$n * \bar{X}$ = -0.913895

Step 6

$b = \bar{Y} - n * \overline{X} = \bar{Y} - Step\ 6 =$ **3.398596**

$\boldsymbol{b = \log_{10} K}$

Step 7

$K = 10^b$ = 2503.779385

K= 2503.78

Step 7a

X1.1.3 The calculations for the standard deviation:

$\frac{(S_{xy})^2}{S_{xx}} = \boldsymbol{Step5 * Step2}$ =0.041885 see X1.3

Step 8

$\boldsymbol{S_{yy} = \sum Y^2 - \frac{(\sum Y)^2}{N}}$ = 0.043305

Step 9

$S_y^2 = \frac{Step\ 9 - Step\ 8}{N-2}$ =4.73E-04

Step 10

$S_n^2 = \frac{Step\ 10}{Step\ 4}$ = 3.17E-03

Step 11

$S_n = \sqrt{Step\ 11}$ =5.63E-02 Standard Deviation

$S_n = \sqrt{Step\ 11}$ =5.63E-02 Standard Deviation

$S_b^2 = S_y^2\left(\frac{1}{N} + \frac{\overline{X^2}}{S_{xx}}\right) = \text{Step 10}\left(\frac{1}{N} + \frac{\overline{X^2}}{\text{Step 4}}\right) =$ **0.009535838**

Step 12

$S_b = \sqrt{Step\ 12} =$ **9.77E − 02** Standard Deviation